RESEARCH ARTICLE

Comparative Analysis of High Impedance Fault Detection Techniques on Distribution Networks

ESTER HAMATWI [ID][1], (Member, IEEE), **ỌDUNAYỌ IMORU** [ID][1,2], (Senior Member, IEEE), **MATHEUS M. KANIME**[1], **AND HITILA S. A. KANELOMBE**[1,3]

[1]Department of Electrical and Computer Engineering, University of Namibia, Oshakati 9000, Namibia
[2]Department of Electrical and Electronic Engineering, University of Johannesburg, Johannesburg 2006, South Africa
[3]HSK Architects and Engineering cc, Outapi 9000, Namibia

Corresponding author: Ester Hamatwi (esterhamatwi@gmail.com)

ABSTRACT This study focused on comparing the performance of three high impedance fault detection techniques for the case of a distribution network to select the technique that is best suited for detecting faults in this network. The three most common techniques; discrete Fourier transform, discrete wavelet transform, and the power spectrum among other techniques were selected for the research work based on literature. The distribution network was modelled in MATLAB/Simulink, along with the High Impedance Fault condition. These fault detection techniques were modelled and applied separately to the distribution network under different operating conditions: high impedance fault, load switching, and normal operation. The suitability of these techniques for the distribution network is evaluated by comparing them in terms of accuracy, processing time, and fault detection margin. The power spectrum technique was found to be the most suitable technique for detecting high impedance faults on a distribution network, with a 100% accuracy, a shorter processing time, and a larger fault detection margin.

I. INTRODUCTION

Detection of High Impedance Faults (HIFs) on distribution networks is a long-standing problem for electrical engineers. An HIF is a type of fault that occurs on a distribution network when an energized overhead conductor touches a high impedance surface or poorly conducting surfaces such as tree branches, rocks, sand, gravel, asphalt, and concrete [1], [2], [3]. HIFs can be classified into two main types: active and passive.

Active HIF occurs when an overhead conductor breaks and touches a highly resistive ground, creating an immediate transient arc [4]. In this regard, the broken conductor touches the ground directly.

Passive HIF occurs when the conductor indirectly comes into contact with a grounded object either through a failure of the conductor mounting system, insulation failure, i.e., the

deterioration of the insulation of an underground conductor over a while, or inadvertent contact with some external elements such as tree branches [5].

An HIF typically produces a small fault current due to the high impedance that is introduced within the current path [1]. These HIF currents are characterized by low magnitudes and they fluctuate in nature hence, they are comparable with normal load currents and are often confused with the increase or decrease in load current [2]. Therefore, the fault currents associated with HIFs are very low such that they cannot trip the protection devices, and hence, they are insufficient to be detected by conventional overcurrent protection devices, such as fuses reclosers, and protection relays [4], [6], [7].

A. HAZARDS AND CONSEQUENCES OF HIFS

The most distinctive feature of HIFs is arcing, which poses a great danger to people and animals by exposing them to electric shocks [8], [9]. HIFs are identified as the second major

cause of death related to distribution networks in Brazil [10]. Specifically, in 2013 and 2014, HIFs resulted in 30 and 53 deaths in Brazil, respectively [11]. Moreover, HIFs are the major causes of wildfires worldwide [12]. In 2009, an incident occurred in Victoria, Australia, whereby HIFs were responsible for five of the Black Saturday bushfires which caused high economic losses and led to more than 170 deaths and the injury of many other people [13]. Furthermore, the electric utility was determined to be responsible for at least 17 of 21 fatal wildfires that occurred in Northern California in 2017, whereby it was confirmed that nearby trees that came into contact with a power line initiated the wildfire [14]. According to [12], the wildfires caused by power lines are highly destructive and larger than the fires caused by other means. Figure 1 illustrates the consequences of an energized conductor falling on wet ground and contacting tree branches.

(a)

(b)

FIGURE 1. High impedance fault due to (a) downed conductors on wet ground/grass and (b) conductors in contact with tree branches [15].

Since HIFs cannot be detected by the overcurrent protection devices, in most cases, the distribution utilities can only detect HIFs based on customers' calls. In this regard, the energized cables can remain bouncing on the ground for a prolonged period thus leading to adverse danger effects, until maintenance crews de-energize the affected branch [10]. In this regard, HIFs can jeopardize the reliability and power quality of the utility due to the possible unplanned service interruption. As such, the indices such as the System Average Interruption Duration Index and the System Average Interruption Frequency Index can increase [4], [6]. HIFs can also result in equipment damage which poses a threat to the facility's assets and may cause irreparable damage associated with high economic losses and could also result in

legal issues. Given these hazards, this highlights the need for more reliable solutions to identify and locate HIFs on distribution grids, using advanced HIF detection techniques.

B. CHARACTERISTICS OF HIFS

The HIFs exhibit characteristics which differentiate them from normal short circuit faults. The characteristics as presented in literature are illustrated in Figure 2 and explained in more detail as follows [4], [9], [10], [17]:

Low current magnitude: the magnitude of the HIF current is lower than the pickup currents of overcurrent protection devices because of the high impedance at the fault point.

Asymmetry: The fault current has different peak values for the positive and negative half-waves. Whereas the positive current half-wave is larger in magnitude than the negative half-wave, mainly caused by the silica present on the contact surfaces.

Non-linearity: The voltage-current curve is nonlinear, resulting from the different resistivity values of the several layers of the contact surfaces.

Intermittent arching: This is associated with low harmonics and noises in the measurement signals. The energized wire usually interrupts the contact with the soil during cycles. This results in the extinction and reignition of the electric arc.

Buildup: The magnitude of the fault current gradually increased to its maximum value in approximately tens of cycles due to a smaller effective initial contact between the conductor and the highly resistive surface.

Shoulder: The fault current increased gradually during several cycles, and eventually reached its steady state condition.

Random behaviour: The resistance at the fault point is large and presents stochastic characteristics. Therefore, HIF behaves differently under different conditions and surfaces since the varying fault path results in a change in the HIF current magnitude from cycle to cycle.

From the HIF's characteristics presented above, it is worth noting that the current resulting from a HIF exhibits a different behaviour and magnitude depending on the contact surface. For instance, for asphalt or dry sand, there will almost be no-fault current [12]. However, for some surfaces such as wet ground, the current magnitude would be quite high, although still below the tripping value of conventional protective devices. This electric arc, which results from the dielectric rupture of the air between the energized conductor and the contact surface, leads to dynamic and distinctive features on the fault current waveform [10]. Considering that different contact surfaces have different resistivity values, the waveform would exhibit different characteristics, such as non-linearity and asymmetry, for different contact surfaces. There might be some changes in HIF contents and magnitudes as the surface moisture evaporates due to the generated heat resulting from the HIF [12]. Moreover, the ground surface material during different seasons can result in different fault current waveforms.
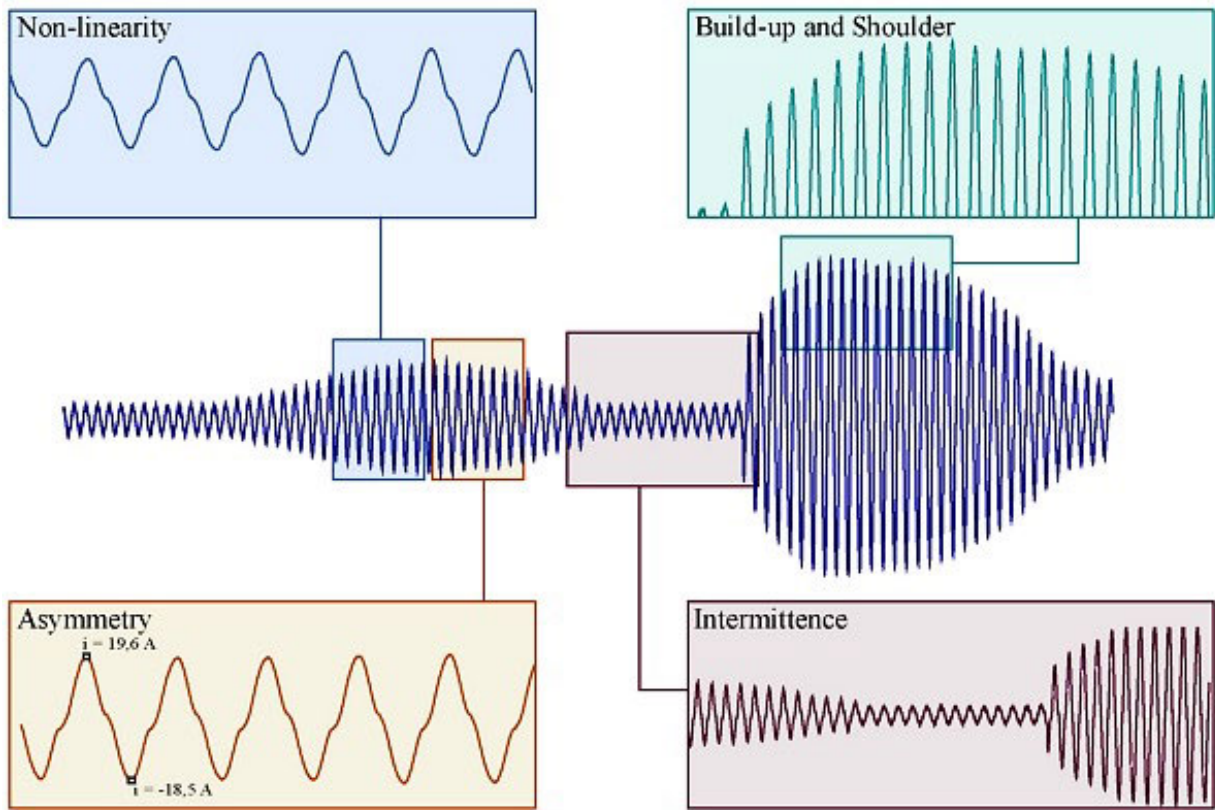
FIGURE 2. Characteristics of currents associated with high impedance faults [4].
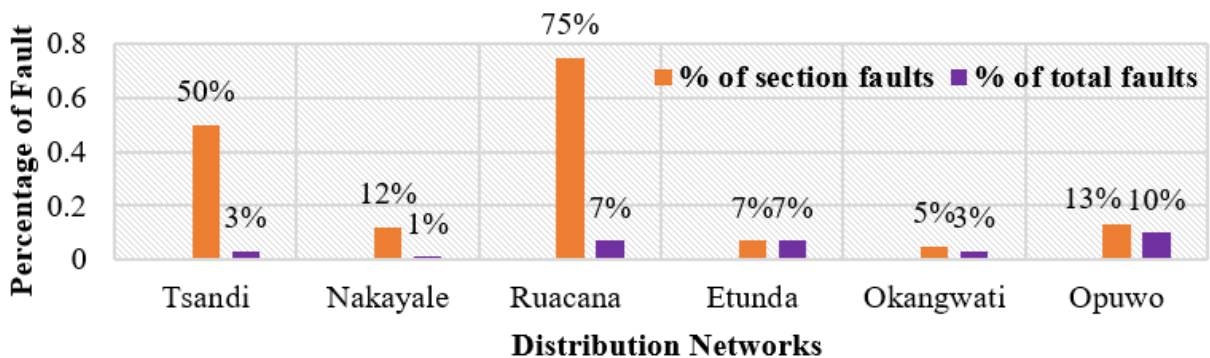

FIGURE 3. Percentage of high impedance faults occurring in the NORED's distribution networks due to downed conductors [16].

C. HIFS ON THE RUACANA MV DISTRIBUTION NETWORK

According to the northern regional electricity distributor (NORED)'s network study report for July 2019 [16], Ruacana's distribution network has the highest percentage of sectional faults due to broken poles and downed conductors compared to the other distribution networks for zone 1. Figure 3 indicates the percentage of total faults and section faults for the distribution networks in zone 1. The factor contributing to the high number of pole breakages in this area compared to other areas in northern Namibia is mainly because Ruacana is mountainous, and windy for most of

the year. As such, poles break thus causing the conductors to sag and touch poorly conducting materials such as the asphalt of the road, grass, and sand, to mention a few. These HIFs can remain on the network without being detected until someone sees the conductors on the ground and contacts the utility personnel.

The detection of HIFs promptly has become an area of considerable interest and prompted a wide range of studies aimed at developing advanced HIF detection techniques [18], [19], [20], [21], [22], [23], [24], [25]. In past investigations, researchers have made a great effort to attempt to

develop effective methods of detecting and isolating HIFs on distribution networks. However, distribution networks have different characteristics and hence, it is recommended to develop and test a technique on the specific network on which it will ultimately be implemented, thereby ensuring accuracy in the HIF detection process.

Eldin et al. [23] used the discrete wavelet transform as a powerful signal-processing tool to extract the details related to the HIF condition in a medium voltage distribution modelled in MATLAB/Simulink. An investigation by Kujur et al. [22] presented a technique for detecting HIFs in a distribution system with distributed generators (DGs) based on residual power as an input. The proposed technique could accurately discriminate between a non-fault and HIF fault condition, even in the presence of DGs. Lai et al. [26] and Torres et al. [25] presented a practical pattern recognition-based technique for detecting HIFs. The technique is based on using the Discrete wavelet transform (DWT) to recognize the distortion in the voltage and current waveforms due to the arcs associated with HIFs. The study by Baqui et al. [24] focused on using a combination of wavelet transform and artificial neural networks to detect HIFs in electrical distribution feeders.

Despite the large number of studies conducted on the detection of HIFs in distribution networks, the researchers in these investigations mainly focused on adopting individual techniques to detect HIFs in the distribution networks, with no performance comparisons made. However, making performance comparisons of various detection techniques on the same network to ultimately select the technique that is best suited for the application is paramount, and thus it is the focal point of this paper. Specific to this study, there is a need to identify an efficient and reliable HIF detection technique for Ruacana's MV distribution network. Therefore, this study focuses on identifying a suitable HIF detection technique for this network through a performance comparison of the existing and most promising HIF detection techniques. Such a technique would ultimately supplement the low impedance fault (LIF) detection devices in detecting HIF on the network to improve the reliability of the distribution network by minimizing unplanned outages and ensuring the safety of the people and animals residing in the vicinity of the network.

The techniques that are normally used for detecting HIFs and have proven to have excellent performance, according to the literature, have been considered in this study [1], [6], [27], [28], [29], [30], [31], [32], [33], [34], [35]. These are: discrete wavelet transform (DWT) [1], [31], signal processing [6], decision tree (DT) [32], fuzzy logic (FL) [33], discrete Fourier transform (DFT) [34], and the power spectrum (PS) technique [20], [35]. To narrow down the investigation, a selection criterion based on the decision matrix will be adopted to compare the techniques and select the three techniques that are recorded to have a higher score than the others, for further investigation and testing. To facilitate the investigation, the MV distribution network of Ruacana and

the three techniques will be modelled in MATLAB/Simulink. Thereafter, a comparison between the three techniques will be carried out by running simulations, under the following operating conditions: normal operation, during an HIF condition, and load switching condition. In each scenario, the performance of each technique will be evaluated by taking note of the following performance factors: accuracy, processing time, and fault detection margin. Finally, the most suitable technique will then be selected for the case of the Ruacana's medium voltage distribution network.

In this regard, the paper is structured as follows. Section II presents a brief review of the established HIF detection techniques as adopted from the literature. Section III presents the concept of the decision matrix that has been used to select the most suitable techniques (three, among others) for further investigation and testing on Ruacana's MV distribution network. Section IV presents the algorithms and MATLAB/Simulink models of the three selected techniques that will be used to detect the HIFs in Ruacana's MV distribution network. Section V presents the MATLAB/Simulink model of Ruacana's MV distribution network, the HIF model using the Emmanuel Model, and the testing, and evaluation of the three HIF detection techniques: DWT, DFT, and PS. Finally, the conclusions and recommendations for future works are drawn in section VI.

II. REVIEW OF ESTABLISHED HIF DETECTION TECHNIQUES
A. MECHANICAL-BASED HIF DETECTION TECHNIQUES
1) ALUMINIUM ROD METHOD
One type of mechanical HIF detection method uses a pendulum that is mounted on an aluminium rod with hooked ends. It is suspended from an under-built neutral conductor to catch the falling conductor and produces a low impedance ground fault then the conventional overcurrent protection will operate upon detection of the ground fault. According to Wester [36], two units are mounted per span, which can be quite costly for application on distribution networks with long feeders such as Ruacana's distribution network. This mechanical method serves to detect most, if not all the sagging conductors that do not touch the earth or a grounded object. In [36], it was mentioned that ice, wind, and tree growth could cause false HIF detection.

B. ELECTRICAL-BASED HIF DETECTION TECHNIQUES
1) FUZZY LOGIC (FL)
Naveh et al. [33] proposed a technique for detecting HIF on the distribution network based on a fuzzy-logic scheme. The proposed fuzzy unit was trained by data from a simulation of distribution systems under different fault conditions. Figure 4 presents the fuzzy logic algorithm structure.

The processing block generates the input patterns from the voltages and current signals as depicted in Figure 4. Samples of the residual current Ir and voltage V_r signals are
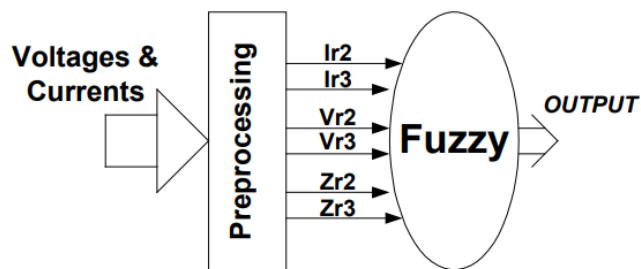
FIGURE 4. Fuzzy logic algorithm structure [33].

then obtained. In the same vein, the second and third harmonics of these signals are obtained using the full cycle discrete Fourier transform (DFT) algorithm from voltage and current samples. The second and third harmonics of the apparent impedance of the faulted distribution line are calculated using (1) [33]:

$$Z_r = \left| \frac{V_r}{I_r} \right| \qquad (1)$$

The results of the performance study showed that the proposed algorithm has a good performance in detecting HIF with non-linear arcing resistance. However, it is tedious to develop fuzzy rules and membership functions, since it requires considerable data and expertise to develop a fuzzy system.

2) DECISION TREE (DT)

Sheng and Rovnyak [32] proposed a HIF detection method based on decision trees (DTs). The DT-based method detects HIF using well-known features, namely, phase current (in rms), the magnitudes of the second, third, and fifth harmonics, and the phase of the third harmonics [32] Simulations were performed using EMTP software on the radial distribution system. The proposed technique yielded excellent results in detecting HIFs and it is associated with low cost since the only measurements required are the current signals for each phase [32]. However, there are drawbacks associated with this technique, such as inaccuracy and instability, such that small changes can lead to large changes in the structure of the optimal decision tree. The fault detection algorithm using DTs is illustrated in the flow chart in Figure 5.

3) DISCRETE WAVELET TRANSFORM (DWT)

Chakraborty et al. [31] proposed a wavelet transform-based approach to detect and classify different shunt faults that may occur in transmission lines. The algorithm is mainly based on calculating the RMS values of the wavelet coefficients of current signals at both ends of the transmission line over a moving window length of half-cycle.

Chen et al. [37] also investigated the detection of HIFs using the discrete wavelet transform (DWT). DWT is a multi-resolution transform that provides high-frequency resolution for low frequencies and high time resolution for high frequencies [38]. The DWT is a series of processes of filtering
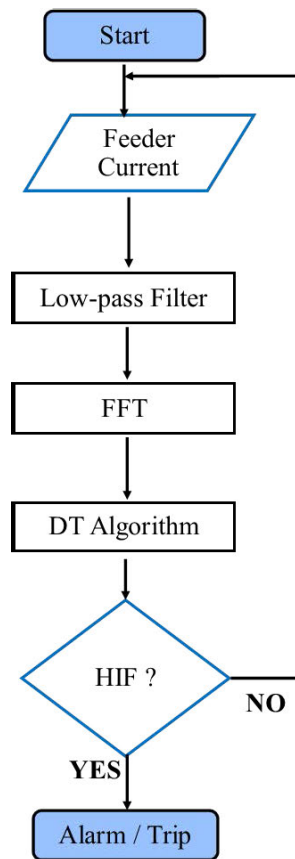

FIGURE 5. Flowchart of the decision tree-based HIF detection algorithm [32].

and down-sampling of the input signal. Scaling functions and wavelet functions are used to achieve this. Given a certain sampled signal $s(n)$, the DWT decomposes it onto several wavelet signals; an approximation signals a_n and n detail signals d_j [26]. The approximation coefficient, which represents the signal's low-frequency components is obtained from a low pass filter and the detail coefficients, which represent the signal's high-frequency components, are obtained using the high pass filter as shown in Figure 6.

If F_s (in *samples/second*) is the sampling frequency used to capture the signal $x(n)$, then the detail space d_j contains the information concerning the components of the signal whose frequencies fall within the interval given by (2), where $k = 1 : n_f$, where n_f is the minimum number of decomposition levels given by (3) [26]. The approximation space a_n includes the low-frequency components of the signal that fall in the interval given by (4):

$$f(d_j) \in [2^{-(k+1)} \cdot f_s, \, 2^{-k} \cdot f_s] \qquad (2)$$

$$n_f = integer \left[\frac{\log \frac{f_s}{f}}{\log(2)} \right] \qquad (3)$$

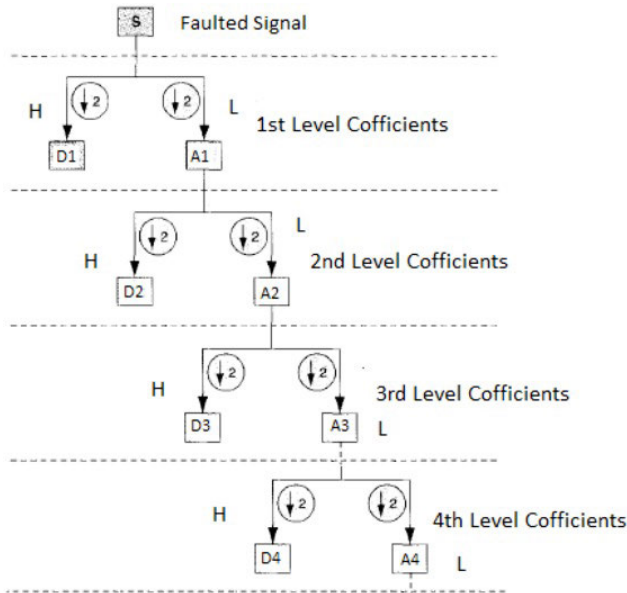$$f(a_n) \in [0, \, 2^{-(n+1)} \cdot f_s] \qquad (4)$$

FIGURE 6. Decomposition of the four-level discrete wavelet transform algorithm [31].

In the investigative presented by Chen et al. [37], the DWT technique was performed for the network under the following conditions:

- Normal Conditions.
- Fault due to inrush current.
- HIF due to the conductor on the tree branch.
- HIF due to the conductor on leaves.
- HIF due to the conductor on the soil.
- Disturbances are due to capacitor switching.

It was observed that the DWT technique could discriminate HIF conditions from normal load currents and transient switching currents. However, one of the shortcomings is the difficulty in identifying the type of disturbance on the network by looking at the DWT waveforms. The procedural approach employed in this study to detect the HIF through the decomposition of signals using the DWT technique will be covered in the subsequent section IV.

4) POWER SPECTRUM (PS)

Wali et al. [35] proposed an HIF detection technique based on the power spectrum (PS). The proposed technique can recognize HIF from any likely case on the feeder with high accuracy and less time than other methods [35]. In this technique, the fast Fourier transform (FFT) is used for decomposition and for extracting the signals of HIF and other power system incidents. PS is defined as the time signal computed using the function given by (5):

$$PS = \frac{1}{N} \Sigma_{n=0}^{N} (X(n))^2 \qquad (5)$$

where N is the number of samples and $X(n)$ is the signal extracted by FFT. The proposed algorithm that is used to

disclose HIF and to discriminate them from other natural events in the feeder comprises of three stages [35];

- Data collection on the feeder.
- FFT is used to extract the signals of the faulted phase.
- The PS technique is used to discriminate the HIF from other cases in the feeder.

Therefore, current signals are used to obtain the characteristics of HIF, whereby the FFT is used for signal extraction, thereafter, the extracted signals are then applied to the PS equation in (5), to detect HIF conditions directly and distinguish them from other events. Figure 7 has been extracted from [35], presenting the PS levels in a distribution network.

It is observed that the PS amplitudes in the HIF region are greater than 0.025, while those in the no-fault region are less than 0.005. The detection level was set to 0.005, and hence, if the PS amplitude becomes greater than 0.005 then a HIF is present, otherwise, there is no HIF present. The results of this technique showed that the technique had 100% accuracy in detecting HIF.

5) DISCRETE FOURIER TRANSFORM (DFT)

Zhibang [34] proposed a technique for detecting HIFs in electrical distribution systems based on observing the harmonic content in the one-sided amplitude spectrum of the impedance. The proposed HIF detection technique can distinguish HIF events from other non-fault events with current waveforms that are similar to HIF current waveforms. In this investigation, the one-sided amplitude spectrum of the impedance was monitored for the network under four scenarios: no disturbances, load switching, capacitor switching, and HIF events. The simulation results for these scenarios have demonstrated that, for the non-fault events, the impedance amplitude values at the location of the harmonics always keep decreasing as the order of the harmonics increases [34]. On the other hand, for the HIF events, the impedance amplitude at the location of the harmonics does not always keep decreasing as the order of the harmonics increases, but fluctuates, up and down.

III. SELECTION OF THE MOST SUITABLE HIF DETECTION TECHNIQUES

The five electrical-based HIF detection techniques that have been discussed in the preceding section have been considered due to their excellent performance as presented in the literature. These techniques all use different approaches to detecting HIFs on the network. However, to narrow down the investigation, further comparisons have been made among the five techniques. In this case, a decision matrix was utilized to select the most suitable three techniques for the distribution network of Ruacana. Using a decision matrix is a recommended procedure for concept selection in modelling and programming, instead of hand-picking techniques. The decision matrix facilitates the selection of an appropriate HIF detection techniques through the process of scoring different categories of these techniques to ascertain that
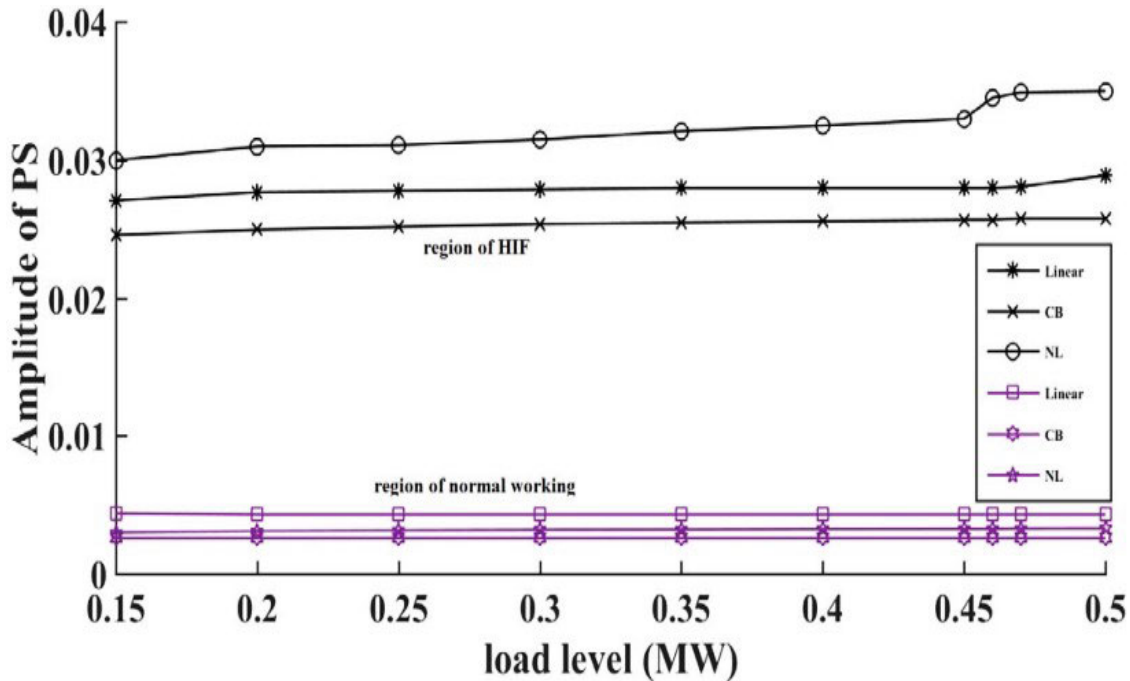
FIGURE 7. High impedance fault detection levels using the power spectrum algorithm [35].

TABLE 1. Performance factors used to rate the selection criterion used in the decision matrix.

Performance	Rating
Much worse than the requirement	1
Worse than the requirement	2
Same as the requirement	3
Better than the requirement	4
Much better than the requirement	5

a desirable tradeoff is ensured, in terms of the following selection criterion:

- Finiteness and definiteness of the technique
- The practicality of the technique
- Level of complexity in the implementation of the technique in industrial applications.

Each criterion is then rated using the concept presented in Table 1.

The decision matrix used to select the three most effective electrical-based HIF detection techniques is summarized in Table 2. Table 2 follows the fundamental principle of concept selection to determine the most suitable HIF detection algorithms for further analysis. In this regard, the performance of the six HIF detection algorithms as per literature reviews has been compared to the set requirements, under different selection criteria. As illustrated in Table 2, each selection criterion is weighted depending on its level of importance, i.e., considering what would make a technique ideal for detecting HIFs effectively. The performance of each technique is then scored against these weights to determine whether it has met the requirements or not, as per the ratings given in Table 1.

Table 2 shows that the three techniques that scored more than others and hence were selected using the decision matrix are:

- Discrete wavelet transform (DWT) with a total score of 72.
- Power spectrum (PS) with a total score of 71.
- Discrete Fourier transform with a total score of 68.

Therefore, these techniques are to be implemented on the model of Ruacana's MV distribution network to detect HIF conditions.

It is worth noting that fewer techniques have been selected depending on the time constraints; it would require time to master, model, and analyse the distribution network using each of these techniques. Therefore, it is necessary to only focus on the most promising techniques (as per their score) and maximize obtaining substantial results from the HIF detection process while using these three techniques. To evaluate which HIF detection method is most suitable, these techniques will be compared in terms of accuracy, processing time, and fault detection margin.

IV. ALGORITHMS OF THE SELECTED HIF DETECTION TECHNIQUES
A. DISCRETE WAVELET TRANSFORM (DWT) HIF DETECTION ALGORITHM
1) DWT-BASED HIF DETECTION ALGORITHM
The Discrete wavelet transform (DWT) HIF detection algorithm adopted in this investigation utilizes the residual voltage and current components to discriminate against normal load and faulted system scenarios. To ensure fault selectivity, the residual decision criteria are qualified with the phase

TABLE 2. Decision matrix used to select the electrical-based HIF detection techniques.

		Electrical-based HIF detection techniques									
		\multicolumn{2}{c}{*FL*}	\multicolumn{2}{c}{*DFT*}	\multicolumn{2}{c}{*PS*}	\multicolumn{2}{c}{*DT*}	\multicolumn{2}{c}{*DWT*}
Selection Criteria	**Weight**	Score	Net Weight	Score	Net Weight	Score	Net Weight	Score	Net Weight	Score	Net Weight
Input & Output	4	5	20	2	8	3	12	3	12	4	16
Finiteness	2	1	2	4	8	5	10	5	10	4	8
Definiteness	3	2	6	5	15	4	12	2	6	3	15
Effectiveness	5	1	5	5	25	5	25	2	10	5	25
Practical implementation	4	1	4	2	12	3	12	3	12	2	8
Total			**37**		**68**		**71**		**48**		**72**

harmonic characteristics. The residual component of the system can be defined with (6) and (7) as follows:

$$V_r = V_a + V_b + V_c \qquad (6)$$
$$i_r = i_a + i_b + i_c \qquad (7)$$

where V_r is the residual voltage, V_a, V_b, and V_c are the instantaneous phase voltages, i_r is the residual current, and i_a, i_b, and i_c are the instantaneous phase currents.

The residual voltages and residual currents are calculated from the phase voltages and current by finding the vector magnitude of all phases. These data, i.e., phase voltages, line currents, residual voltage, and currents, are then passed into a 200-dataset buffer that results in outputs a 200 units array of data streams. The data stream is then passed through a 1-D 3rd order Daubechies wavelet decomposition function which returns an approximation coefficient and three levels of detailed coefficients.

The number of decomposition levels n_f is determined by the low-frequency components to be traced; the lower the frequency components to be extracted, the higher the number of decomposition levels of the DWT [26]. The number of decomposition levels is dependent on the sampling frequency as well as the frequency of the power supply. For this investigation, the three-level DWT decomposition has been adopted owing to its capability of yielding adequate results in terms of an improved resolution.

Figure 8 presents a typical three-level DWT decomposition structure. The HIF is classified by the magnitude offset of the level 2 and level 3 detailed coefficients.

These two levels defined higher-order harmonics discriminated by the detector's sampling frequency. The frequency ranges of the 2nd and 3rd detailed coefficients are given by (8) and (9), respectively:

$$\frac{F_s}{2} > F_{cD2} \geq \frac{F_s}{4} \qquad (8)$$
$$F_s \geq F_{cD3} \geq \frac{F_s}{2} \qquad (9)$$

where F_s is the detector's sampling frequency, F_{cD2} and F_{cD3} are level 2 and level 3 frequencies, respectively.

The magnitude offset of each detailed coefficient is calculated as the logarithmic value of the detailed coefficients' standard deviations using (10):
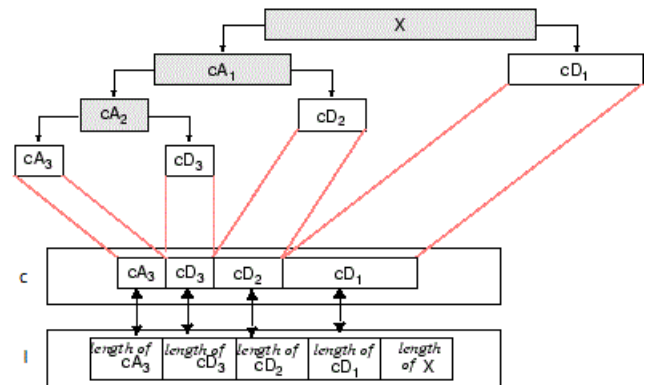
$$Offset = log(std(cD_n)) \qquad (10)$$

FIGURE 8. Three-level discrete wavelet transform decomposition [40].

The diagnosis conclusion of the DWT-based HIF detection algorithm is made as follows; if the offset exceeds 0, i.e., the standard deviation exceeds 1, a high impedance alarm is issued to the controller. This alarm remains ON for a specified period defined by the protection engineer, before issuing a final circuit breaker trip command. The pickup time delay gives the operator time to act. For interlocking purposes, the alarm or trip is not issued when the circuit breaker is open or when other faults, such as overcurrent have been detected. The flowchart in Figure 9 illustrates the procedures for implementing the DWT-based HIF detection algorithm.

2) DWT-BASED HIF DETECTION MODEL
The detailed HIF detection model is presented in Figure 10, consisting of the DWT blocks and other functionalities. The model has been implemented in MATLAB/Simulink and it operates following the procedures illustrated in the flow chart in Figure 9. In this regard, the residual current and voltage signals are computed and then fed into the discrete wavelet transform block. The discrete wavelet transform decomposes the residual signals into a three-level decomposition of approximate and detailed coefficients. The offset values are then calculated by taking the logarithmic value of the detailed coefficient's standard deviation.

During a high impedance fault event, the offset value is expected to be greater than zero, and a high impedance fault alarm signal is issued. Under normal operating conditions, the
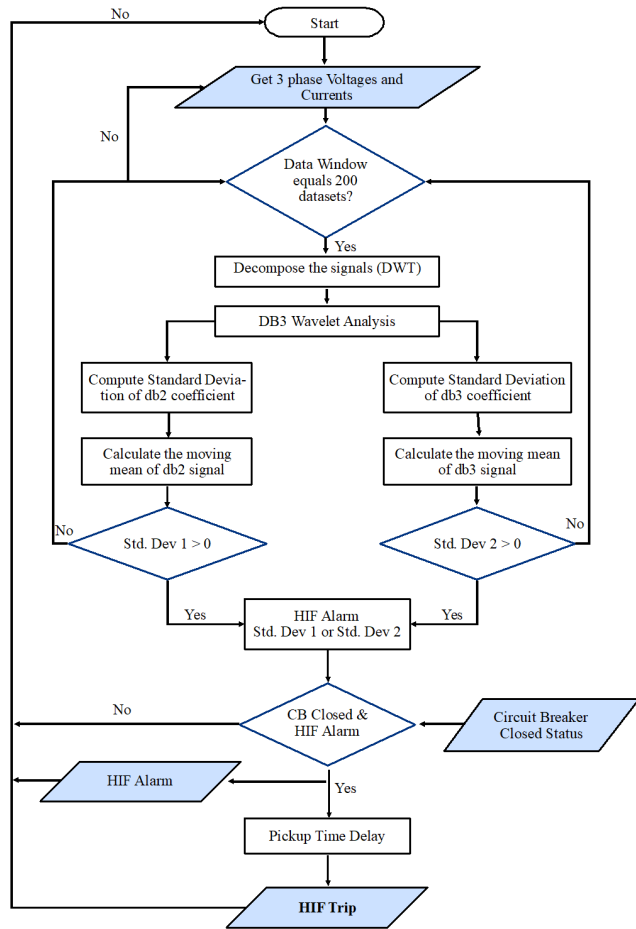
FIGURE 9. Flowchart of the discrete wavelet transform-based HIF detection algorithm.

offset value is expected to remain below zero. The JK flip-flop with a clock frequency of $5kHz$ is used to maintain the status of the relay after it has issued a trip signal to the breaker until an operator resets the relay by pressing the target reset button.

B. POWER SPECTRUM (PS) HIF DETECTION ALGORITHM
1) PS-BASED HIF DETECTION ALGORITHM
This technique is based on the analysis of the power spectrum (PS) of the current signals to determine whether there is HIF on the feeder [35]. Under this technique, current signals are obtained from the feeder to calculate the residual current. The residual current is then transformed into the frequency domain using fast Fourier transform (FFT). Thereafter, the PS of the residual signal under normal conditions is determined. This enables the determination of a threshold value by finding the maximum value on the residual current's power spectrum (PS) curve for the network under normal running conditions. The diagnosis conclusion is made such that, if the PS value becomes greater than the threshold value, then an HIF exists on the network/feeder. The flowchart in Figure 11 summarises the PS-based HIF detection algorithm.

2) PS-BASED HIF DETECTION MODEL
The PS-based HIF detection algorithm was modelled in MAT-LAB/Simulink to perform the functions that are outlined in the flowchart in Figure 11.

C. DISCRETE FOURIER TRANSFORM (DFT) HIF DETECTION ALGORITHM
1) DFT-BASED HIF DETECTION ALGORITHM
The DFT-based HIF detection technique is based on the analysis of the harmonic content in the impedance amplitude of a feeder to determine whether there is an HIF condition on the feeder. This technique was adopted by Zhibang et al. [34], to identify the harmonic impedance behaviour and distinguish HIFs from other non-fault events namely, load switching and other conditions that behave like an HIF condition.

The steps for implementing the DFT-based HIF detection technique are as follows:

- **Step 1:** Measure the time-domain current $i(t)$ and voltage $v(t)$ signals at the beginning of the feeder.
- **Step 2:** Apply DFT to the current $i(t)$ and voltage $v(t)$ waveforms to transform them from time-domain to frequency-domain $i(f)$ and $v(f)$.
- **Step 3:** Obtain the one-sided amplitude spectrum of the current $|i(f)|$ and of the voltage $|v(f))|$ signals.
- **Step 4:** Obtain the one-sided amplitude spectrum of the impedance $|Z(f)|$ which is calculated using (11).

$$|Z(f)| = \frac{|v(f)|}{|i(f)|} \qquad (11)$$

- **Step 5:** Diagnosis Conclusion: Under the normal condition, the amplitudes of the one-sided spectrum of the impedance $|Z(f)|$ remain constant. However, if a disturbance occurs, the amplitude tends to increase or decrease, accordingly. Whereby, if the values/amplitudes of $|Z(f)|$ at the location of harmonics keep decreasing as the order of harmonic increases then it is not an HIF event. Otherwise, it is an HIF event.

The flowchart in Figure 12 illustrates the procedures for implementing the DFT-based HIF detection algorithm.

2) DFT-BASED HIF DETECTION MODEL
The DFT-based HIF detection algorithm was modelled in MATLAB/Simulink as shown in Figure 13 to perform the functions that are outlined in the flowchart in Figure 12.

From Figure 13, the phase currents and voltage signals from the feeder are transformed from the time domain to the frequency domain using the Fast Fourier Transform (FFT) block. The one-sided amplitude spectrum of both the current and the voltage in the frequency domain is then obtained using the absolute value block. Thereafter, the one-sided amplitude spectrum of the impedance is calculated using the division block, in accordance with (11). The output of the division block is then observed to identify whether there was an HIF on the network or not, by keeping track of the trend of the impedance amplitudes as the harmonic orders increase.
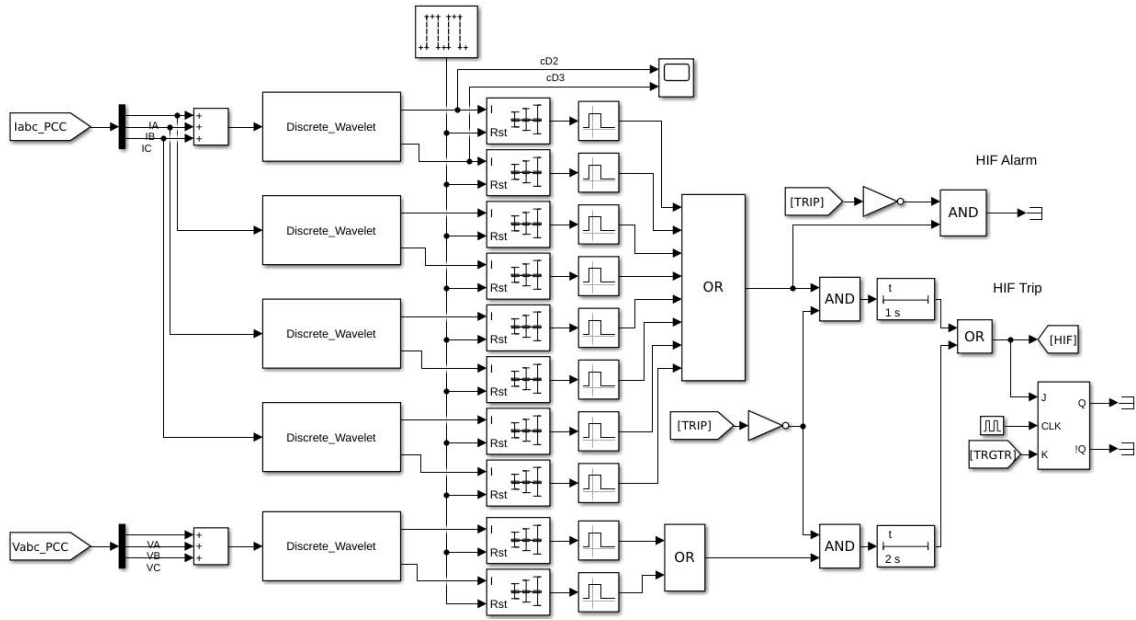
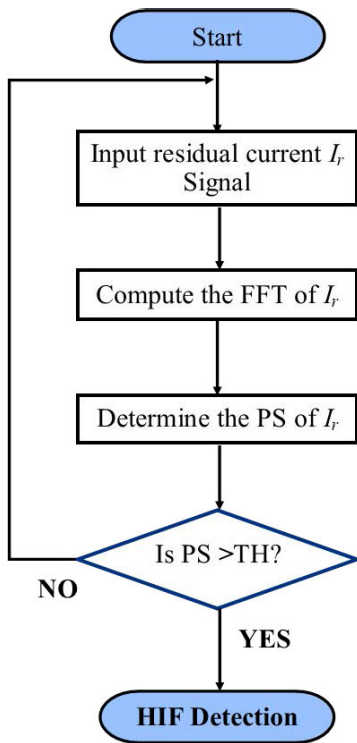**FIGURE 10.** MATLAB/Simulink model of the discrete wavelet transform-based HIF detection algorithm.

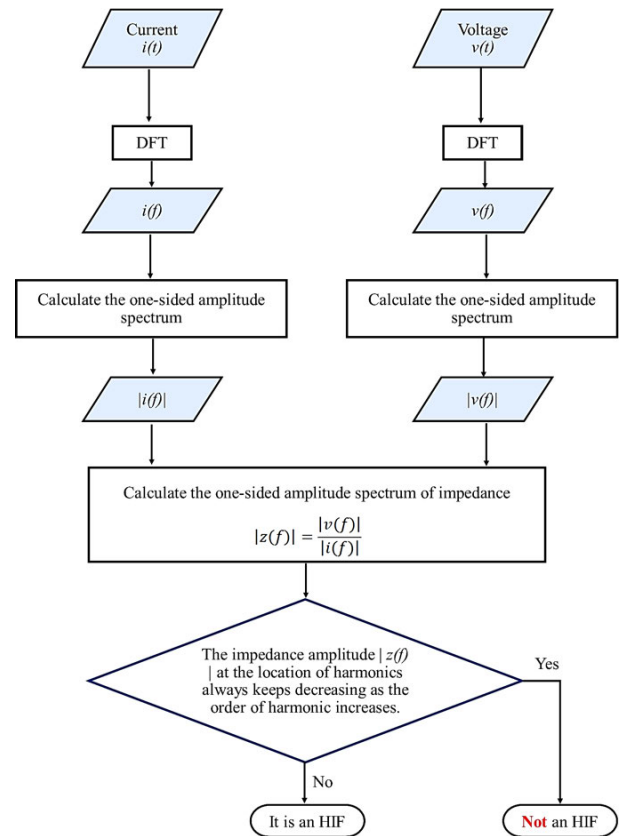**FIGURE 11.** Flowchart of the power spectrum-based HIF detection algorithm.

FIGURE 12. Flowchart of the discrete fourier transform-based HIF detection algorithm.

V. RESULTS AND DISCUSSIONS

A. HIF MODEL

The simplified Emmanuel model which was proposed by Lai et al. [26] has been adopted in this investigation to emulate an HIF fault condition. Figure 14 presents the model, implemented in MATLAB/Simulink.

Table 3 presents the parameters of the simplified Emmanuel model used in this investigation to emulate the HIF on Ruacana's MV distribution network.
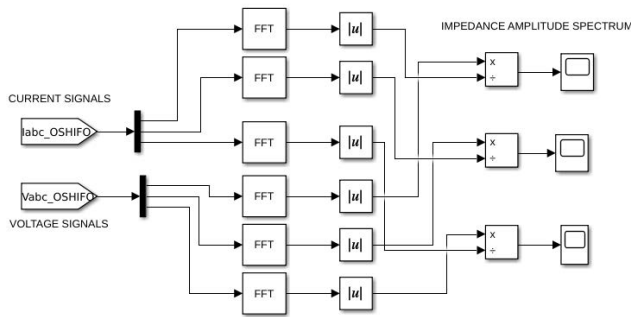
FIGURE 13. MATLAB/Simulink model of the discrete fourier transform-based HIF detection algorithm.
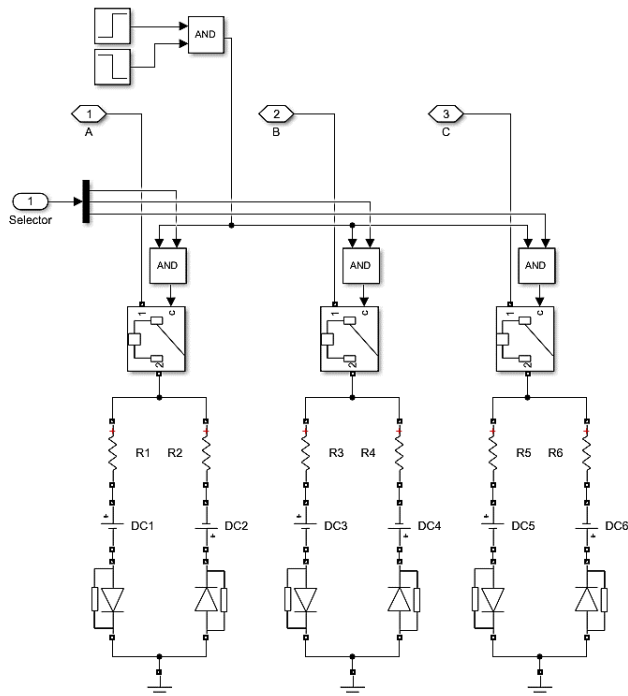

FIGURE 14. MATLAB/Simulink model of the high impedance fault (simplified Emmanuel model).

TABLE 3. Parameters of the high impedance fault model (simplified Emmanuel model).

Parameter	Value
$R1$	$1.44kW$
$R2$	$1.27kW$
$DC1$	$6.092kW$
$DC1$	$4.91kW$

The model consists of two DC sources representing the inception voltage of air in the soil and/or between trees and the distribution line. The two unequal resistances, $R1$ and $R2$, represent the fault resistances and the unequal values can generate asymmetric fault currents. When the phase voltage is higher than the positive DC voltage $DC1$, the fault current flows towards the ground. On the other hand, when the phase voltage is lower than the negative DC voltage $DC2$, the fault

current reverses. For values of the phase voltage between $DC1$ and $DC2$, no fault current flows [26].

B. RUACANA MV DISTRIBUTION NETWORK MODEL

Figure 15 presents the MATLAB/Simulink model of Ruacana's MV distribution network. The distribution network considered in this investigation has a voltage level of 11kV. The distribution grid has been tapped from the national grid through a 50MVA, 50Hz, 66/11kV step-down transformer. There are several distribution transformers which further step down the voltage to 400V (3 phase) and 230V (single phase) to feed the respective load centres.

The DWT, DFT, and PS HIF detection techniques have been performed on the network under these scenarios:

- Scenario 1: Normal conditions,
- Scenario 2: During a HIF condition and
- Scenario 3: Under load switching.

C. DISTRIBUTION NETWORK FEEDER UNDER NORMAL CONDITIONS

The operating principles considered under this scenario are such that the distribution network operates to supply power to 26 basic load centres with ratings ranging from $150kW$ to $10kW$. These load centres exclude the load centre that will be switched during scenario 2. Moreover, the HIF model (simplified Emmanuel model) shown in Figure 14 is disconnected from the model during this scenario and the parameter used for the normal operating condition are given in Table 4.

TABLE 4. Parameters used for the normal operating condition.

Parameter	Status	Switching time (s)
Load Centres ($1-27$)	Supplied (except 1 load centre which will be switched in under scenario 2)	0
HIF model	Deactivated	—

1) DISCRETE WAVELET TRANSFORM

Figure 16 presents the waveforms of the detailed coefficients $cD2$ and $cD3$ which are obtained from the DWT-based HIF detection model presented in Figure 10.

It is observed from Figure 16 that the offset values fluctuate between $-5dB$ and $-16dB$, which is below 0, and hence this shows that the feeder is under normal conditions.

2) POWER SPECTRUM TECHNIQUE

Figure 17 presents the power spectrum (PS) amplitude and the rotational operator under normal conditions. In this context, the relational operator is an output from the comparator, which compares the power spectrum amplitude obtained under a particular operating condition to the PS under the normal condition, i.e., the threshold value. Hence, when the new PS is greater than the threshold PS, the output from the comparator would be true, and the plot of the relation operator would step up from zero to one, else it will remain zero.
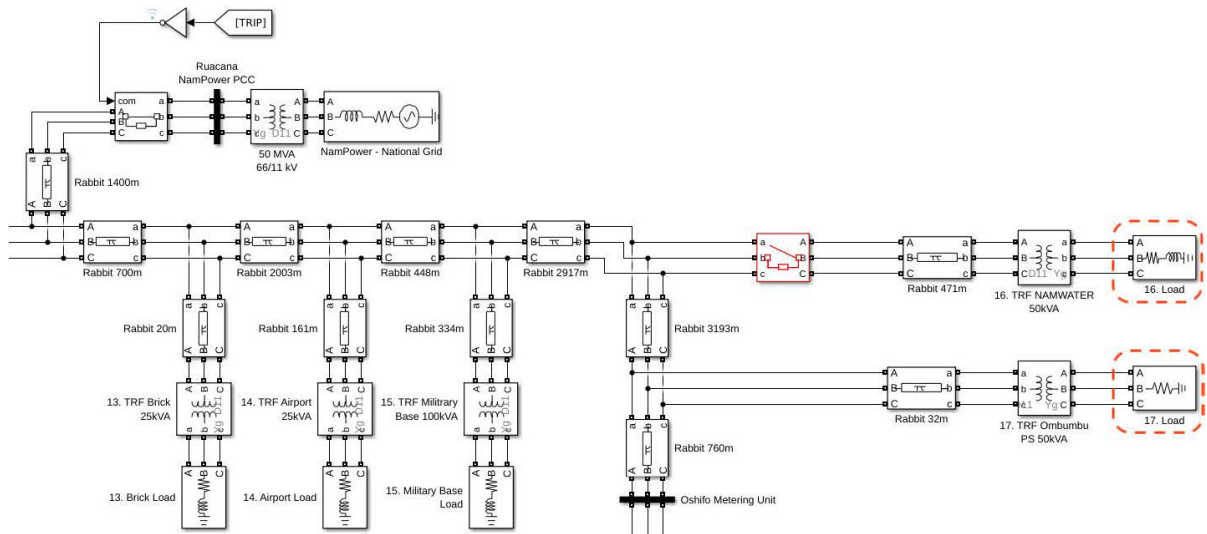
FIGURE 15. MATLAB/Simulink model of the medium voltage distribution network: Oshifo main feeder (Northern Namibia).
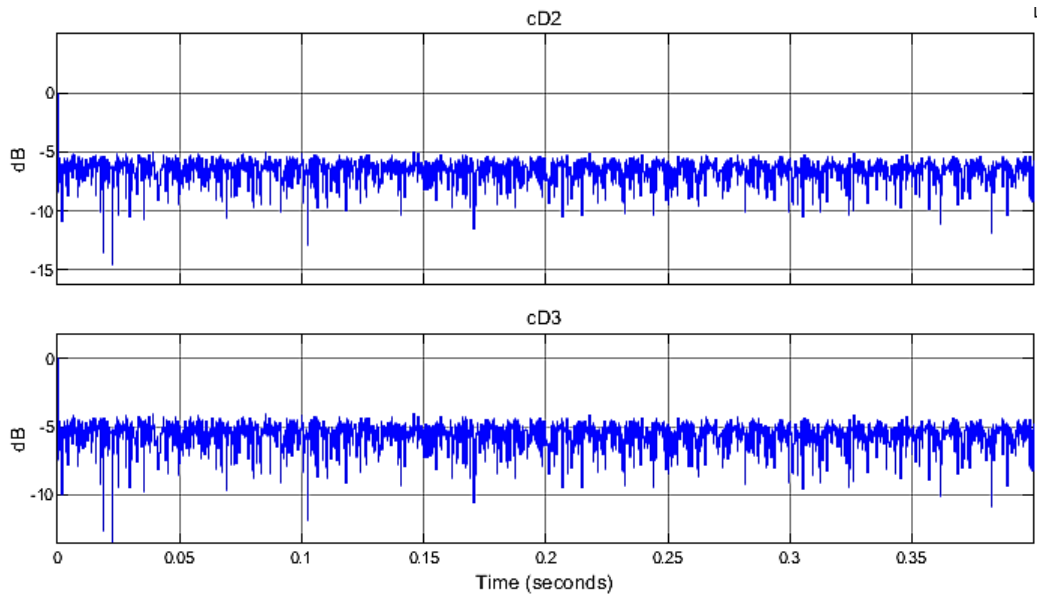

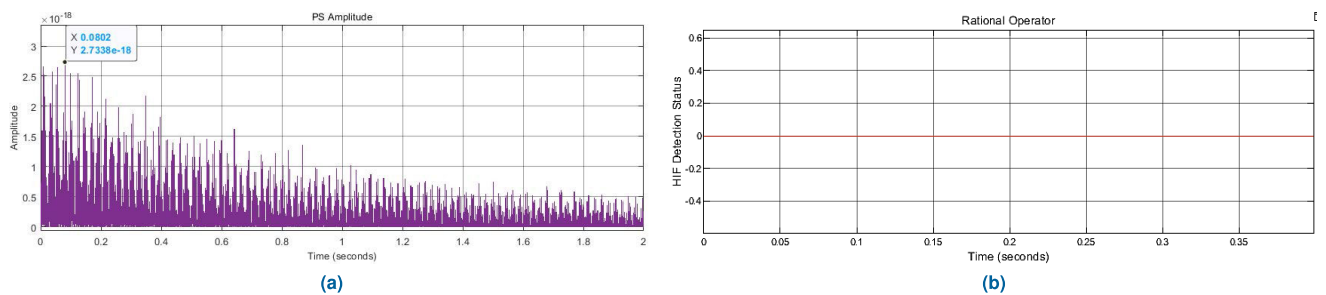**FIGURE 16.** Waveforms of the detailed coefficients cD2 and cD3 under normal operating condition.

FIGURE 17. Normal conduction plot for (a) power spectrum amplitude and (b) rotational operator.

It is observed that the highest amplitude of the power spectrum is 2.7×10^{-18}, which is equivalent to $-17.57 dB$ on the logarithm scale. This is the threshold value on the PS

spectrum, that will be compared to other PS values under the different operating conditions and make a diagnostic conclusion. The rational operator remains constant at 0, under
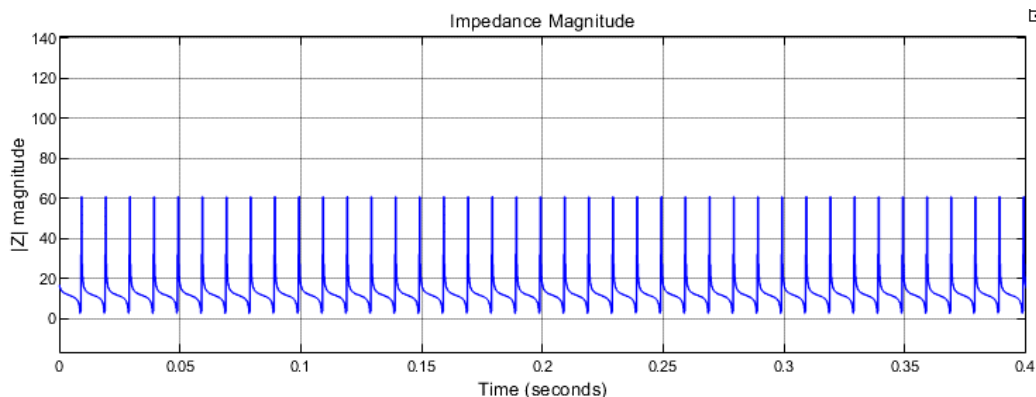
FIGURE 18. One-sided amplitude of the impedance under normal operating condition.

TABLE 5. Parameters used for the load switching condition.

Parameters	Status	Switching time (s)
Load centre 16	$10kW$	0.1
Load centre 17	$25kW$	0.1
HIF model	Deactivated	–

TABLE 6. Parameters used for the HIF condition.

Parameter	Status	Switching time (s)
Load Centres $(1-27)$	Supplied (except 1 load centre which will be switched in under scenario 2)	0
HIF model	Activated	0.4

normal operating conditions, meaning that the amplitude of the power spectrum is below the set threshold value.

3) DISCRETE FOURIER TRANSFORM
Figure 18 presents the one-sided spectrum of the impedance, obtained using the DFT-based HIF detection model. It is observed that the one-sided spectrum has a maximum constant amplitude of 60Ω. The amplitude of the one-sided impedance is neither increasing nor decreasing under normal conditions, and this indicates that there are no disturbances on the feeder.

D. LOAD SWITCHING CONDITION ON THE DISTRIBUTION NETWORK FEEDER
The load switching scenario has been realized in simulation by using two loads as shown in Figure 15 which were set to switch on after $0.1s$. Table 5 shows the magnitude of the loads and their corresponding switching times.

1) DISCRETE WAVELET TRANSFORM
Figure 19 presents the waveforms of the detailed coefficients $cD2$ and $cD3$ under the load switching condition. During load switching conditions, the offset waveforms have reduced from $-5dB$ and started to fluctuate between $-8dB$ and $-14dB$. However, since the waveforms are still below 0, the DWT diagnosis technique regards this as a non-HIF event.

2) POWER SPECTRUM TECHNIQUE
Figure 20 presents the power spectrum (PS) amplitude and the rotational operator under the load switching condition. During the load switching event, the highest PS amplitude

was recorded to be 4.4×10^{-22}, which is equivalent to $-21.36\,dB$. However, it is still below the set threshold value of 2.7×10^{-18}, hence it is regarded as a non-HIF event. Likewise, the rational operator remains constant at zero.

3) DISCRETE FOURIER TRANSFORM
Figure 21 shows the one-sided spectrum of the impedance, for the load switching condition. There is no significant change observed in the amplitude of the impedance compared to when the system was operating under normal conditions. Except for the amplitude slightly fluctuating above and below 60Ω, thus this is not characterized as an HIF event.

E. HIF CONDITION ON THE DISTRIBUTION NETWORK FEEDER
The operating principles considered under this scenario are presented in Table 6. The distribution network supplies all load centres and the HIF condition gets activated at $0.4s$.

1) DISCRETE WAVELET TRANSFORM
Figure 22 presents the waveforms of the $cD2$ and $cD3$ coefficients. The HIF condition was activated at $0.4s$. From Figure 22, it is observed that as the HIF condition is activated at $0.4s$, the waveforms of the detailed coefficients $cD2$ and $cD3$ increase to $10dB$, a value that is greater than zero. Hence, this is considered a HIF event.

2) POWER SPECTRUM TECHNIQUE
Figure 23 presents the PS amplitude and the rotational operator under the HIF condition. From Figure 23a, it is observed
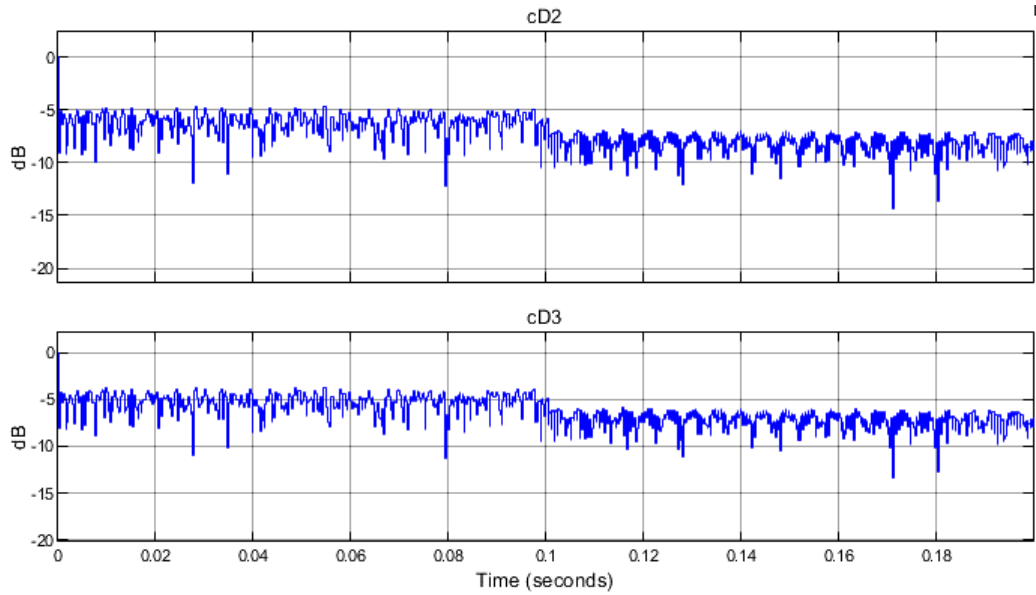
FIGURE 19. Waveforms of the detailed coefficients cD2 and cD3 under the load switching condition.
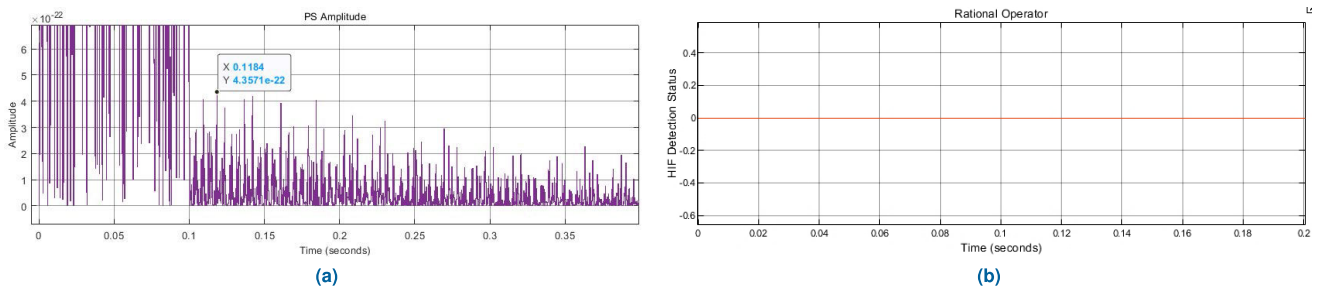

FIGURE 20. Load switching condition plots for (a) power spectrum amplitude and (b) rotational operator.
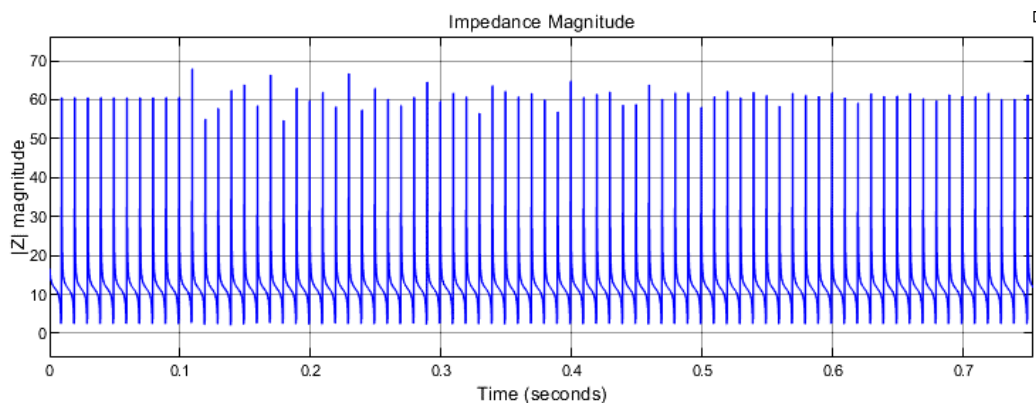

FIGURE 21. One-sided amplitude of the impedance under the load switching condition.

that the maximum peak of the PS amplitude is 2.2×10^{-7}, which is greater than the set threshold value of 2.7×10^{-18}. Moreover, the rational operator in Figure 23b changed from 0 to 1 when an HIF event occurred at 0.4s. Therefore, this is regarded as an HIF event.

3) DISCRETE FOURIER TRANSFORM
Figure 24 presents the one-sided spectrum of the impedance. During an HIF fault event, the amplitude of the one-sided spectrum increased to 120Ω. An increase in the one-sided amplitude is regarded as a HIF event.
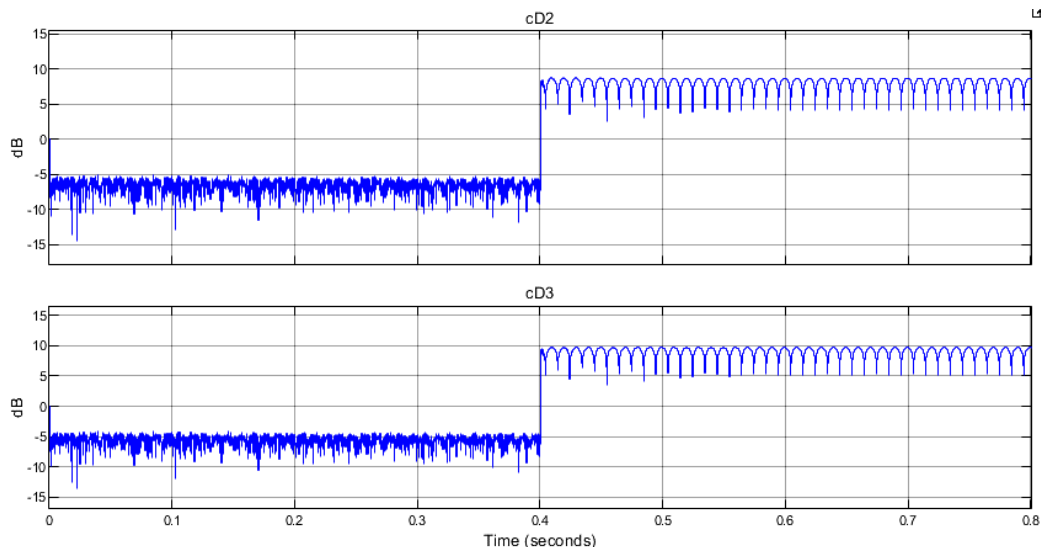
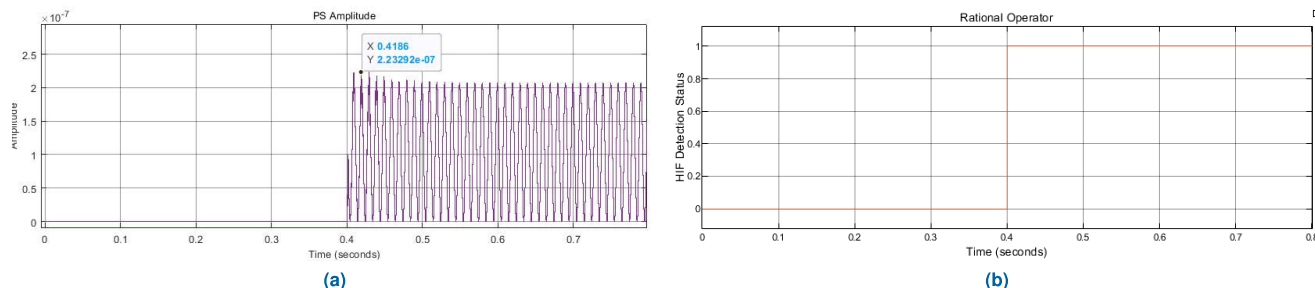**FIGURE 22.** Waveforms of the detailed coefficients cD2 and cD3 under the high impedance fault condition.

FIGURE 23. High impedance fault condition plot for (a) Power spectrum amplitude and (b) rotational operator.
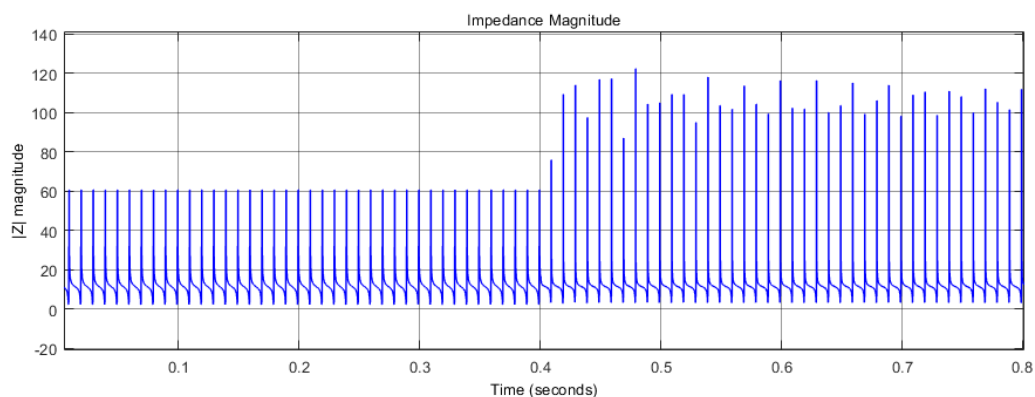

FIGURE 24. One-sided amplitude of the impedance under the high impedance fault condition.

F. COMPARING THE PERFORMANCE OF THE HIF DETECTION TECHNIQUES

In power system protection, there are pre-determined factors that are used to evaluate the performance of conventional fault detection devices. These are also referred to as the general properties that a protective system should possess.

These factors include selectivity, sensitivity, accuracy, reliability and dependability, and speed [39]. The most reliable HIF detection algorithm among the three, i.e., DWT, DFT, and PS is determined by comparing the three factors that are specifically related to the investigation of this paper. Thus, under normal conditions, during load switching, and under
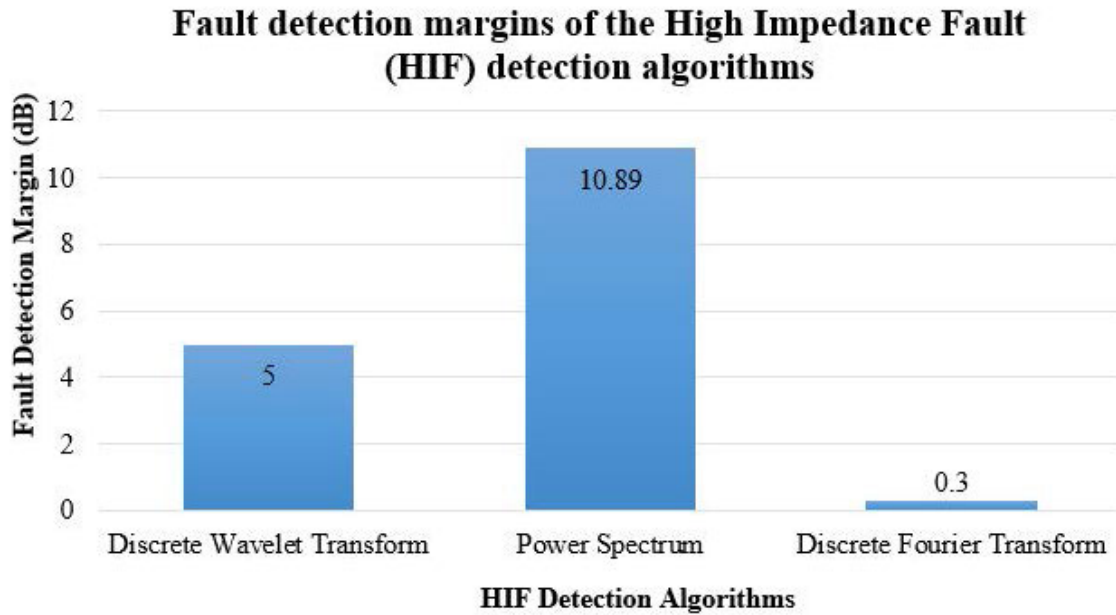
FIGURE 25. Fault detection margins of the high impedance fault detection algorithms.

an HIF event, the following factors; the accuracy, processing time (speed) and fault detection margin (sensitivity) of the three techniques were compared.

1) ACCURACY
Accuracy can be defined as the ability of the technique to accurately discriminate an HIF event from other system disturbances such as load switching. Based on the results presented earlier, the three techniques all gave good performance results in terms of accuracy since they managed to discriminate the HIF events from load switching. Therefore, the techniques are rated 100% in terms of accuracy.

2) PROCESSING TIME
In this context, the processing time refers to the time taken for the technique to detect the presence of an HIF event on the system. A shorter processing time means that the technique can detect HIFs in a shorter period as compared to other techniques. In this investigation, the processing time for each technique was recorded and the average was taken. Table 7 presents the processing times of the DWT, DFT, and PS techniques, over four trials, and the average processing time in minutes.

TABLE 7. Processing times of the high impedance fault detection techniques.

Technique	Trial 1	Trial 2	Trial 3	Trial 4	Avg time (min)
DWT	2.34	2.37	2.43	2.35	2.37
DFT	2.12	2.21	2.19	2.23	2.18
PS	1.45	1.53	1.47	1.35	1.45

From Table 7, it is observed that the PS-based HIF detection technique has the shortest processing time as compared

to the other two techniques. Therefore, it is considered to detect the HIF at a faster rate, thus making it reliable compared to the DWT and DFT techniques, in terms of the response time.

3) FAULT DETECTION MARGIN
The fault detection margin is referred to as the range of values over which the technique discriminates HIF from other disturbances in the system. A larger HIF detection margin means that the chances of the technique falsely detecting other fault events on the feeder as HIF is very low as compared to the other two techniques.

The fault detection margin (FDM) is obtained using (12):

$$FDM = |log_{10}(TH) - log_{10}(TON)| \qquad (12)$$

where TH is the threshold value and TON is the techniques' output values for the system under normal operating conditions.

In this investigation, the fault detection margins of the DWT, DFT, and PS HIF detection algorithms are computed as follows: For the DWT technique, the values are already expressed in terms of logarithms; hence these values are used directly in (12) to determine the FDM.

Considering a threshold value of zero (0) and $TON = -5dB$ from Figure 16, the FDM of the DWT-based HIF detection technique is $5dB$ as deduced from (13).

$$|0 - (-5)| = 5dB \qquad (13)$$

For the PS-based HIF detection technique, considering a threshold value of 2.2×10^{-7}, and a $TON = 2.7 \times 10^{-18}$ from Figure 17, the FDM is $10.89\ dB$ as deduced from (14)

using (12).

$$|log_{10}(2.2 \times 10^{-7}) - log_{10}(2.7 \times 10^{-18})| = 10.89 \, dB \tag{14}$$

whereas for the DFT-based HIF detection technique, considering a threshold of 120; and a *TON* = 60 from Figure 18, the *FDM* is 0.3*dB* as deduced from (15) using (12).

$$|log_{10}(120) - log_{10}(60)| = 0.3dB \tag{15}$$

Figure 25 gives a graphical representation of the fault detection margins of the three HIF detection algorithms.

Based on this comparison, it is observed that the DFT technique has the lowest HIF detection margin of 0.3*dB*, while DWT has a HIF detection margin of 5*dB*, and the PS technique has the largest detection margin of 10.89 *dB*. Therefore, the power spectrum (PS) technique has been proven to be the most suitable technique for detecting HIFs in terms of the HIF detection margin.

VI. CONCLUSION

This research investigation focused on the detection of HIFs on Ruacana's MV distribution network (DN) which has been identified to have a higher percentage of HIFs due to broken poles and downed conductors as compared to the other distribution networks in zone 1 of the NORED's network in Namibia. The detection of HIFs on the DN of Ruacana was performed using three techniques namely, DWT, PS, and DFT.

To evaluate which HIF detection method is most suitable for Ruacana's MV network, these techniques were compared in terms of accuracy, processing time, and fault detection margin. The three techniques were rated 100% in terms of accuracy because they managed to discriminate the HIF events from other system disturbances such as load switching. In terms of processing time, the PS technique was observed to have the shortest processing time of 1 minute and 45 seconds, compared to the other two techniques. This means that the PS technique can detect the faults in a shorter period than other techniques thereby making it more responsive. Concerning the fault detection margin, the PS technique was determined to have the largest detection margin of 10.89 *dB*. This makes it the most suitable technique for detecting HIFs in terms of the HIF detection margin. Overall, it can be concluded that the PS technique is the most responsive and reliable technique for detecting HIFs on Ruacana's MV distribution network.

REFERENCES
[1] A. R. Adly, R. A. E. Sehiemy, A. Y. Abdelaziz, and N. M. A. Ayad, "Critical aspects on wavelet transforms based fault identification procedures in HV transmission line," *IET Gener., Transmiss. Distrib.*, vol. 10, no. 2, pp. 508–517, Feb. 2016.
[2] A. Ghaderi, H. L. Ginn, III, and H. A. Mohammadpour, "High impedance fault detection: A review," *Electr. Power Syst. Res.*, vol. 143, pp. 376–388, 2017.
[3] A. V. Masa, J.-C. Maun, S. Werben, and A. Siemens, "Critical aspects on wavelet transforms based fault identification procedures in HV transmission line," in *Proc. 17th Power Syst. Comput. Conf. (PSCC)*, vol. 10, 2016, pp. 508–517.

[4] A. Aljohani and I. Habiballah, "High-impedance fault diagnosis: A review," *Energies*, vol. 13, no. 23, p. 6447, Dec. 2020, doi: 10.3390/EN13236447.
[5] J. Vico, M. Adamiak, C. Wester, and A. Kulshrestha, "High impedance fault detection on rural electric distribution systems," in *Proc. IEEE Rural Electr. Power Conf. (REPC)*, Orlando, FL, USA, May 2010, pp. 3–8, doi: 10.1109/REPCON.2010.5476205.
[6] G. N. Lopes, V. A. Lacerda, J. C. M. Vieira, and D. V. Coury, "Analysis of signal processing techniques for high impedance fault detection in distribution systems," *IEEE Trans. Power Del.*, vol. 36, no. 6, pp. 3438–3447, Dec. 2021, doi: 10.1109/TPWRD.2020.3042734.
[7] S. Chakraborty and S. Das, "Application of smart meters in high impedance fault detection on distribution systems," *IEEE Trans. Smart Grid*, vol. 10, no. 3, pp. 3465–3473, May 2019.
[8] É. M. Lima, R. D. A. Coelho, N. S. D. Brito, and B. A. D. Souza, "High impedance fault detection method for distribution networks under nonlinear conditions," *Int. J. Electr. Power Energy Syst.*, vol. 131, Oct. 2021, Art. no. 107041.
[9] É. M. Lima, N. S. D. Brito, and B. A. D. Souza, "High impedance fault detection based on stockwell transform and third harmonic current phase angle," *Electr. Power Syst. Res.*, vol. 175, Oct. 2019, Art. no. 105931.
[10] É. M. Lima, C. M. S. Junqueira, N. S. D. Brito, B. A. Souza, R. A. Coelho, and H. G. M. S. de Medeiros, "High impedance fault detection method based on the short-time Fourier transform," *IET Gener., Transmiss. Distrib.*, vol. 12, no. 11, pp. 2577–2584, Jun. 2018.
[11] W. C. Santos, F. V. Lopes, N. S. D. Brito, and B. D. Souza, "High-impedance fault identification on distribution networks," *IEEE Trans. Power Del.*, vol. 32, no. 1, pp. 23–32, Feb. 2017.
[12] O. A. Gashteroodkhani, M. Majidi, and M. Etezadi-Amoli, "Fire hazard mitigation in distribution systems through high impedance fault detection," *Electr. Power Syst. Res.*, vol. 192, Mar. 2021, Art. no. 106928.
[13] B. Teague, S. Pascoe, and R. McLeod, "The 2009 Victorian bushfires royal commission final report: Summary," Victorian Bushfires Roy. Commission, VIC, Australia, Tech. Rep., Aug. 2010, vol. 4. [Online]. Available: https://apo.org.au/node/22187
[14] A. Robertson, "Investigators confirm that PG & E power lines started the deadly camp fire," The Verge, Washington, DC, USA, Tech. Rep., May 2019. [Online]. Available: https://www.theverge.com/2019/5/15/18626819/cal-fire-pacific-gas-and-electric-camp-fire-power-lines-cause
[15] M. Sedighizadeh, A. Rezazadeh, and N. I. Elkalashy, "Approaches in high impedance fault detection a chronological review," *Adv. Elect. Comput. Eng.*, vol. 10, no. 3, pp. 114–128, 2010.
[16] *Network Studies Report*, EMCON, Windhoek, Namibia, 2019.
[17] F. B. Costa, B. A. Souza, N. S. D. Brito, J. A. C. B. Silva, and W. C. Santos, "Real-time detection of transients induced by high-impedance faults based on the boundary wavelet transform," *IEEE Trans. Ind. Appl.*, vol. 51, no. 6, pp. 5312–5323, Nov./Dec. 2015.
[18] K. Sarwagya, S. De, and P. K. Nayak, "High-impedance fault detection in electrical power distribution systems using moving sum approach," *IET Sci., Meas. Technol.*, vol. 12, no. 1, pp. 1–8, Jan. 2018.
[19] S. Kavaskar and N. K. Mohanty, "Detection of high impedance fault in distribution networks," *Ain Shams Eng. J.*, vol. 10, no. 1, pp. 5–13, Mar. 2019.
[20] S. Roy and S. Debnath, "PSD based high impedance fault detection and classification in distribution system," *Measurement*, vol. 169, Feb. 2021, Art. no. 108366.
[21] M.-T. Yang, J.-C. Gu, J.-L. Guan, and C.-Y. Cheng, "Detection of high impedance faults in distribution system," in *Proc. IEEE/PES Transmiss. Distrib. Conf. Expo., Asia Pacific*, Apr. 2005, pp. 1–5.
[22] A. P. Kujur and T. Biswal, "Detection of high impedance fault in distribution system considering distributed generation," in *Proc. Int. Conf. Innov. Mech. Ind. Appl. (ICIMIA)*, Bengaluru, India, Feb. 2017, pp. 406–410.
[23] A. H. Eldin, N. Mohamed, and E. Abdallah, "Detection of high impedance faults in medium voltage distribution networks using discrete wavelet transform," in *Proc. 22nd Int. Conf. Exhib. Electr. Distrib. (CIRED)*, 2013, pp. 1–4, doi: 10.1049/CP.2013.0608.
[24] I. Baqui, I. Zamora, J. Mazón, and G. Buigues, "High impedance fault detection methodology using wavelet transform and artificial neural networks," *Electr. Power Syst. Res.*, vol. 81, no. 7, pp. 1325–1333, Jul. 2011.
[25] V. Torres, "High impedance fault detection using discrete wavelet transform," in *Proc. IEEE Electron., Robot. Automot. Mech. Conf.*, Cuernavaca, Mexico, Nov. 2011, pp. 325–329.

[26] T. M. Lai, L. A. Snider, and E. Lo, "Wavelet transform based relay algorithm for the detection of stochastic high impedance faults," *Electr. Power Syst. Res.*, vol. 76, no. 8, pp. 626–633, May 2006.

[27] A. Wontroba, A. P. Morais, G. J. Cardoso, J. P. A. Vieira, P. E. Farias, M. Gallas, and J. P. Rossini, "High-impedance fault detection on downed conductor in overhead distribution networks," *Electr. Power Syst. Res.*, vol. 211, Oct. 2022, Art. no. 108216, doi: 10.1016/J.EPSR.2022.108216.

[28] M. Kavi, Y. Mishra, and M. D. Vilathgamuwa, "High-impedance fault detection and classification in power system distribution networks using morphological fault detector algorithm," *IET Gener., Transmiss. Distrib.*, vol. 12, no. 15, pp. 3699–3710, Aug. 2018, doi: 10.1049/IET-GTD.2017.1633.

[29] M. Wei, H. Zhang, F. Shi, W. Chen, and V. Terzija, "Nonlinearity characteristic of high impedance fault at resonant distribution networks: Theoretical basis to identify the faulty feeder," *IEEE Trans. Power Del.*, vol. 37, no. 2, pp. 923–936, Apr. 2022, doi: 10.1109/TPWRD.2021.3074368.

[30] V. Swarnkar, K. S. Diwan, M. Singh, and S. Ralhan, "Machine learning based high impedance fault diagnosis in microgrid," in *Proc. 2nd Int. Conf. Adv. Electr., Comput., Commun. Sustain. Technol. (ICAECT)*, Apr. 2022, pp. 1–4, doi: 10.1109/ICAECT54875.2022.9807880.

[31] S. Chakraborty, S. Singh, A. Bhalla, P. Saxena, and R. Padarla, "Wavelet transform based fault detection and classification in transmission line," *Int. J. Res. Eng. Appl. Sci.*, vol. 2, no. 5, pp. 1–8, May 2012.

[32] Y. Sheng and S. M. Rovnyak, "Decision tree-based methodology for high impedance fault detection," *IEEE Trans. Power Del.*, vol. 19, no. 2, pp. 533–536, Apr. 2004.

[33] H. Naveh, H. K. Zadeh, B. Hosseini, and A. Zadeh, "A novel approach to detection high impedance faults using fuzzy logic," in *Proc. 39th Int. Universities Power Eng. Conf.*, Bristol, U.K., 2004, pp. 373–376.

[34] L. Zhibang, "High impedance fault detection in power distribution systems with impedance-based methods in frequency domain," M.S. thesis, Electr. Comput. Eng., Univ. British Columbia, Vancouver, BC, Canada, 2013.

[35] M. K. Wali, A. N. Hussain, and W. F. Hani, "High impedance fault detection based on power spectrum technique," in *Proc. Int. Conf. Eng. Technol. (ICET)*, Aug. 2017, pp. 1–6.

[36] C. G. Wester, "High impedance fault detection on distribution systems," in *Proc. Rural Electr. Power Conf.*, 1998, pp. 1–5.

[37] J. C. Chen, B. T. Phung, H. W. Wu, D. M. Zhang, and T. Blackburn, "Detection of high impedance faults using wavelet transform," in *Proc. Australas. Universities Power Eng. Conf. (AUPEC)*, Perth, WA, Australia, Sep. 2014, pp. 1–6.

[38] J. Gao, X. Wang, X. Wang, A. Yang, H. Yuan, and X. Wei, "A high-impedance fault detection method for distribution systems based on empirical wavelet transform and differential faulty energy," *IEEE Trans. Smart Grid*, vol. 13, no. 2, pp. 900–912, Mar. 2022, doi: 10.1109/TSG.2021.3129315.

[39] Y. G. Paithankar and S. Bhide, *Fundamentals of Power System Protection*. New Delhi, India: Prentice-Hall, 2003.

[40] The MathWorks. *Wavedec, 1-D Wavelet Decomposition*. Accessed: Jun. 1, 2022. [Online]. Available: https://www.mathworks.com/help/wavelet/ref/wavedec.html

ODUNAYO IMORU (Senior Member, IEEE) received the B.Eng. degree (cum laude) in electrical and computer engineering from the Federal University of Technology, Minna, Nigeria, in 2005, the M.Sc. degree in electrical engineering from the Delft University of Technology, The Netherlands, in 2010, and the Ph.D. degree in electrical engineering from the Tshwane University of Technology, Pretoria, South Africa, in 2017.

He has over 15 years of lecturing and industrial experience in both Africa and Europe. He is currently a Senior Lecturer with the Department of Electrical and Computer Engineering, University of Namibia (JEDS Campus), Ongwediva, Namibia, and also a Senior Research Associate with the University of Johannesburg, South Africa. His research interests include electrical machines and drives, fault diagnosis and condition monitoring (AI, ML, and DL), and signal processing applications. He was a recipient of many scholarly prizes and presentation awards.

MATHEUS M. KANIME received the B.Eng. (cum laude) and M.Sc. degrees in engineering and technology in the field of electrical engineering from Kazan State Power Engineering University, Russia, in 2008 and 2010, respectively.

Since 2011, he has been a Lecturer with the University of Namibia, teaching different disciplines with the Department of Electrical and Computer Engineering. His research interests include modern electric power and energy systems, power systems protection, and clear-energy technologies and sustainability.

ESTER HAMATWI (Member, IEEE) received the B.Sc. degree in electrical engineering from the University of Namibia, Ongwediva, Namibia, in 2015, the M.Sc. degree in electrical engineering from the University of KwaZulu-Natal, in 2017, and the Ph.D. degree in electrical engineering from the University of Cape Town, in 2023.

She is currently a Lecturer with the Department of Electrical and Computer Engineering, University of Namibia. Her research interests include electrical machines and drives, condition monitoring and fault diagnosis, and power electronic converters and their applications in power systems.

HITILA S. A. KANELOMBE received the B.Sc. degree in electrical engineering from the University of Namibia, in 2020.

He is currently an Electrical Engineer with HSK Architects and Engineering cc, specializing in light system designs and automation. His research interests include the diagnosis of high and low impedance faults in power distribution networks, power system protection, and renewable energy technologies.

• • •